Lamellar Structures Formed by Stratum Corneum Lipids *in Vitro*: A Deuterium Nuclear Magnetic Resonance (NMR) Study

William Abraham[1,2] and Donald T. Downing[1]

Received December 18, 1991; accepted April 22, 1992

Hydrated lipid mixtures consisting of stratum corneum ceramides, cholesterol, specifically deuterated palmitic acid, and cholesteryl sulfate were investigated by solid-state ^2H NMR spectroscopy at different temperatures. The mole ratio of cholesterol to ceramides was varied from 1 to 0. ^2H NMR spectra from these mixtures showed powder patterns with quadrupolar splittings smaller than those obtained from control mixtures containing dipalmitoylphosphatidylcholine (DPPC) instead of the ceramides. This result is attributed to the rigid amide group of the ceramides, with a planar configuration, which could prevent close packing of the α-methylenes of the acyl chains. There was a gradual loss of symmetry in the powder pattern as the amount of cholesterol was decreased and the amount of ceramides (or DPPC) was increased concomitantly. The loss was more pronounced in the ceramide-containing samples. This phenomenon is interpreted as a decrease in the axial reorientation rate of the α-deuterated palmitic acid in the bilayers, presumably caused by the increased hydrogen bonding resulting from the high amount of hydroxyl-bearing ceramides. Spectra obtained at temperatures above 60°C indicated the formation of a hexagonal phase (H_{II}) by the ceramide-containing mixtures. Spectra of the ω-deuterated palmitic acid in the mixture containing 76 mol% ceramides and no cholesterol indicated phase separation into a more rigid phase and a more mobile phase in the temperature range of 25 to 60°C. The bilayer configuration of lipids at 25°C was confirmed by thin-section electron microscopy.

KEY WORDS: stratum corneum; ceramides; ^2H nuclear magnetic resonance (NMR); bilayer; hexagonal phase; hydrogen bonding.

INTRODUCTION

Mammalian stratum corneum (SC) consists of highly cornified cells embedded in an extracellular matrix of lipid lamellae (1). These extracellular membranous structures constitute the major barrier to percutaneous penetration of water and other solutes (2,3). SC lipid bilayers are unique in their composition and contain no phospholipids (4), which are the major bilayer-forming components in other biomembranes. The extracellular lipid lamellae are predominantly made up of ceramides, cholesterol, free fatty acids, cholesteryl sulfate, and small amounts of some less well-characterized nonpolar components (5,6).

The ability of the heterogeneous lipid mixtures of SC to form bilayer structures in the absence of phospholipids has proved somewhat intriguing. Recently, these nonpolar lipid mixtures have been shown to form stable bilayer structures *in vitro* (7–9). While these studies provided information on the morphology of the lipid lamellae formed *in vitro*, there is very little known about the role of individual lipids in maintaining the epidermal barrier function. Some recent investigations using differential scanning calorimetry (10,11), infrared (IR) spectroscopy (12,13), and electron spin resonance (ESR) spectroscopy (14) have provided information on lipid phase transitions in SC lipid lamellae. Freeze-fracture and thin-section electron microscopy (15–17) and X-ray diffraction (18) studies have provided some insight into the bilayer thickness and packing of the lamellar structures of SC. However, information on a molecular level is lacking in these systems. An understanding of the interactions between the component lipid molecules of SC lipid lamellae is essential for a better understanding of the barrier function.

As part of an effort to determine the interactions between component lipid molecules of SC lipid bilayers, we have initiated an investigation using solid-state ^2H NMR spectroscopy, which is ideally suited to investigate the molecular dynamics of lipids in lamellar structures. In this article, we report the results from a ^2H NMR investigation of lipid bilayers made from SC lipids consisting of SC ceramides, cholesterol, cholesteryl sulfate, and specifically deuterated palmitic acid. While this model system resembles SC in its lipid composition, the phase behavior reported in the present study can be taken only as an approximation of the phase behavior of lipids in native SC. The role of any protein matrices, including the effect of corneocyte lipid envelopes on the lipid bilayers, is not considered in the present investigation.

MATERIALS AND METHODS

Lipids. Sheets of SC were prepared by trypsin digestion of pieces of pig epidermis, as described previously (19). SC was dried, weighed, and then extracted in a series of chloroform–methanol mixtures (1:2, 1:1, and 2:1, by volume) for 2 hr in each mixture. The extracts were combined and concentrated using a Rotovap. Ceramides were isolated from the total SC lipid extract by preparative thin-layer chromatography (TLC). For this, the lipid mixture from the total stratum corneum extract was applied on 20 × 20-cm silica gel plates (soft layer Adsorbosil plates, Alltech Associates, Inc., Deerfield, IL) and developed to the top with chloroform:methanol:acetic acid (190:7:1, by volume) and then with hexane:ether:acetic acid (70:30:1, by volume). The plates were dried and scanned under UV light (200 nm) in a photodensitometer (Shimadzu CS-930) to locate the six ceramide bands, which were scraped from the plates together and eluted with chloroform:methanol (2:1, by volume). Cholesterol and synthetic L-α-dipalmitoyl phosphatidylcholine were purchased from Sigma Chemical Co. Cholesteryl sulfate was prepared by reaction of cholesterol with excess chlorosulfonic acid in pyridine and purified chromatographically. Palmitic acids specifically deuterated at the alpha position and at the omega position were purchased from MSD Isotopes (Montreal, Canada). α-CD_2 palmitic acid was re-

[1] Marshall Dermatology Research Laboratories, Department of Dermatology, University of Iowa College of Medicine, Iowa City, Iowa.

[2] To whom correspondence should be addressed at Cygnus Therapeutic Systems, 400 Penobscot Drive, Redwood City, California 94063.

0724-8741/92/1100-1415$06.50/0

crystallized twice from hexane to remove the deuterium source that gave rise to an isotropic signal in the ^2H solid-state spectrum.

Preparation of Lipid Bilayers. Appropriate volumes of solutions of individual lipids in chloroform:methanol (2:1, by volume) were combined to obtain mixtures of the composition shown in Table I. The lipid mixtures were dried under a stream of nitrogen and then under vacuum and were then hydrated in deuterium-depleted water (Aldrich Chemical Co., Milwaukee, WI) to a final concentration of 50% by weight of water and 50% lipid. The mixtures were dispersed with the aid of a glass rod and packed in 5-mm NMR sample tubes that were cut to a length of 3 cm. The sample contained 70–80 mg of lipid in a sample volume of 100–150 μl. The sample tube was then flushed with nitrogen and flame-sealed to prevent any loss of water and any oxidation of lipids during data acquisition in the spectrometer. The lipids were analyzed by thin-layer chromatography after spectral accumulation and there was no indication of oxidation of any of the components. The ceramide-containing samples were incubated at 80°C and the DPPC-containing samples at 65°C for 15 min to assure thermal equilibration and homogenization by diffusion and were then cooled to room temperature before spectral accumulation.

NMR Spectroscopy. ^2H NMR spectra were obtained at 46.07 MHz on a Bruker MSL-300 wide-bore spectrometer using the quadrupole echo pulse sequence (20). Complete phase cycling was used to minimize error due to nonorthogonality and gain imbalance of the receiver channels in the quadrature detection mode. The $\pi/2$ pulse length was 2.6 μsec for the 5-mm solenoid coil. A pulse interval of 18 μsec and a recycle delay of 400 msec were used. Spectra at different temperatures were obtained after equilibrating the samples at the desired temperature in the spectrometer for at least 20 min. Quadrupolar splittings ($\Delta\nu_q$) were measured as the distance between the two horns in the powder pattern spectra. Order parameters were calculated from $\Delta\nu_q$, which follows the relation $\Delta\nu_q = (3/2)QS_{CD}[3\cos^2\delta - 1]/2$ for a randomly dispersed bilayer system, where Q is the static deuterium quadrupolar coupling constant (~170 kHz for C–D bonds in hydrocarbons), S_{CD} is the order parameter of the C–D vector, and δ is the angle between the magnetic field and the bilayer normal (21,22). For acyl chains in bilayers, S_{CD} is a time-average function and measures angular fluctuations of the C–D bond with respect to the director axis of acyl chain. In a powder pattern spectra, the quadrupolar peaks correspond to $\delta = 90°$ (21). Thus $\Delta\nu_q = (3/4)(170)S_{CD}$, or $S_{CD} = \Delta\nu_q/(127.5)$, where $\Delta\nu_q$ is in kilohertz.

Electron Microscopy. After NMR spectral acquisition, small amounts of the hydrated lipid mixtures were fixed in 0.2% RuO_4 in cacodylate buffer for 15 min at room temperature, washed in cacodylate buffer, and preembedded in 1% agar. The samples were then dehydrated in graded acetone, embedded in Spurr's resin, and sectioned. Silver-gold sections were stained with uranyl acetate and lead citrate and examined in a Hitachi H-7000 transmission electron microscope at 75 kV.

Table I. Composition of the Lipid Mixtures Used in the Present Investigation

	Mole percent of[a]				
Mixture	Ceramides	Cholesterol	Palmitic acid	Cholesteryl sulfate	DPPC
1	38	38	19	5	—
2	57	19	19	5	—
3	76	—	19	5	—
4	—	38	19	5	38
5	—	19	19	5	57
6	—	—	19	5	76

[a] The final mixtures were 50% by weight of lipid in water.

RESULTS

The composition of different lipid mixtures that were investigated in the present study is listed in Table I. Mixtures 1–3 contained SC ceramides, cholesterol, deuterated palmitic acid, and cholesteryl sulfate. α-CD_2 palmitic acid and ω-CD_3 palmitic acid were used in separate experiments. Mole ratios of cholesterol to ceramides in the mixtures were changed from 1 to 0 as shown in Table I. Mixture 1, containing 38 mol% of ceramides, 38% cholesterol, 19% palmitic acid, and 5% cholesteryl sulfate, was taken as a close approximation to the *in situ* lipid composition of SC (5,6). In mixtures 4–6 the ceramides were replaced by DPPC, a well-characterized, bilayer-forming lipid used as a control in the present investigation.

α-CD_2 Palmitic Acid. Figure 1 shows the ^2H NMR spectra of α-deuterated palmitic acid intercalated in bilayers made from lipid mixtures listed in Table I. Mixtures 1, 4, and 5 gave symmetric powder patterns, as seen in Figs. 1A, D, and E. Mixtures 2 and 6 gave powder patterns in which the quadrupolar peaks were broad and were not well defined, as seen in Figs. 1B and F, while mixture 3 did not give a symmetric powder pattern (Fig. 1C). $\Delta\nu_q$ and S_{CD} from these spectra are listed in Table II. As the amount of cholesterol was lowered and the amount of ceramides (or DPPC) was

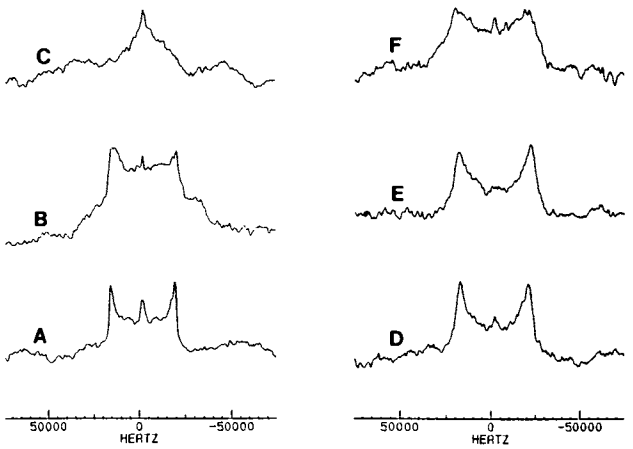

Fig. 1. ^2H NMR spectra of α-CD_2 palmitic acid intercalated in bilayers formed from mixtures shown in Table I. The mixtures were 50% by weight of lipid and 50% water. (A) Mixture 1, number of scans (NS) = 16,000. (B) Mixture 2, NS = 40,000. (C) Mixture 3, NS = 40,000. (D) Mixture 4, NS = 8000. (E) Mixture 5, NS = 16,000. (F) Mixture 6, NS = 32,000. Spectral conditions are described under Materials and Methods.

Table II. Deuterium Quadrupolar Splitting for α-CD_2 Palmitic Acid in the Different Lipid Mixtures

Mixture	Quadrupolar splitting, $\Delta\nu_q$ (kHz)	Order parameter, S_{CD}
1	35.2	0.276
2	35.7	0.280
3	—	—
4	38.6	0.303
5	40.5	0.318
6	41.0	0.322
Palmitic acid	116.7	0.915

increased concomitantly, $\Delta\nu_q$ and S_{CD} increased in both the ceramide- and the DPPC-containing mixtures. Also, the $\Delta\nu_q$ and S_{CD} for the ceramide-containing mixtures were lower than that for the DPPC-containing mixtures. It should be noted that no powder pattern spectra from any of the mixtures were observed until they were heated above their gel–liquid crystalline transition temperature and maintained at that temperature for at least 15 min before cooling to room temperature for spectral acquisition. This suggests that these nonpolar high melting lipids of SC do not form bilayers upon hydration *in vitro,* unless they were equilibrated in a liquid crystalline state first and then cooled to ambient temperature. Figure 2 shows the ^{2}H NMR spectrum of α-CD_2 palmitic acid hydrated in water. $\Delta\nu_q$ and S_{CD} from this spectrum are shown in Table II and indicate that the α-CD_2 in hydrated palmitic acid is in a rigid environment. Spectra obtained from the ceramide-containing mixtures using the α-CD_2 palmitic acid at higher temperatures indicated the formation of a more mobile hexagonal phase, as reported recently (23). The α-CD_2 was found to be labile upon heating and gave rise to an isotropic signal in addition to the quadrupolar peaks, in subsequent NMR experiments. While the α-methylene in an ester-linked acyl chain is stable, the α-methylene in a free fatty acid is acidic and could become labile at higher temperatures. The isotropic peak became stronger after each heating and cooling cycle. The α-CD_2 palmitic acid was therefore not used in subsequent experiments.

ω-CD_3 Palmitic Acid. Figure 3 shows the ^{2}H NMR spectra of ω-CD_3 palmitic acid intercalated in bilayers made from mixtures 1–3 listed in Table 1, at different temperatures. Symmetric powder pattern spectra were obtained for all the mixtures. In the spectra obtained from mixture 1, $\Delta\nu_q$ decreased gradually with increasing temperatures, as seen in Fig. 3A. At 60°C, there was an additional pair of quadrupolar peaks with a $\Delta\nu_q$ of 1.953 kHz, indicating the presence of an additional, more mobile phase. This new phase was shown to be a hexagonal (H_{II}) phase based on ^{2}H NMR and freeze-fracture electron microscopic investigations (23). At 80°C, the quadrupolar peaks gave rise to an isotropic peak.

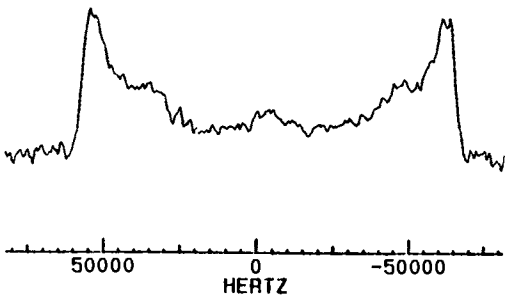

Fig. 2. ^{2}H NMR spectrum of α-CD_2 palmitic acid:water (50:50, by weight). NS = 2200. Spectral conditions are described under Materials and Methods.

Mixture 2 gave a symmetric powder pattern at room temperature. Increasing the temperature gave rise to some interesting changes in the peak shape, as seen in Fig. 3B. The symmetric quadrupolar peaks gave rise to an anisotropic peak around 60°C which became resolved into a pair of quadrupolar peaks with significantly reduced $\Delta\nu_q$ of 1.221 kHz at 70°C and 977 Hz at 80°C. Figure 3C shows the spectra obtained from mixture 3. The room-temperature spectrum corresponded to a gel-phase spectrum which was broad, with a $\Delta\nu_q$ of 16.6 kHz. There was also a broad isotropic peak. As the temperature was raised, the spectrum resolved into a sharp powder pattern with a $\Delta\nu_q$ of 977 Hz at 70°C and 732 Hz at 80°C.

The DPPC-containing mixtures gave rise to symmetric powder pattern spectra and the $\Delta\nu_q$ decreased abruptly from 45 to 60°C due to gel-to-liquid crystalline transition. There was a gradual decrease in the $\Delta\nu_q$ above 60°C. Mixture 6, which contained 76 mol% DPPC and no cholesterol, gave a gel-phase spectrum with a $\Delta\nu_q$ of 12.207 kHz at 25°C. At 45°C, there were two pairs of quadrupolar peaks with $\Delta\nu_q$ of 11.719 kHz and 3.906 kHz, indicating some phase separation. At higher temperatures, this mixture gave only a single pair of quadrupolar peaks. The cause for this apparent phase separation at 45°C in mixture 6 is not clear. The $\Delta\nu_q$ values for mixtures 1–6 at 50% water content are shown as a function of temperature in Figs. 4A and B.

Effect of Water Content. Figures 4C and D show the $\Delta\nu_q$ values as a function of temperature for mixtures 1–6 when the water content in the mixtures was 25% by weight. The most noticeable change on decreasing the water content from 50 to 25% occurred in mixture 3, containing 76 mol% of ceramides and no cholesterol. The room-temperature spectrum was a broad gel-phase spectrum with a pair of quadrupolar peaks, corresponding to a more mobile phase, superimposed on the gel-phase spectrum, as shown in Fig. 5. This pattern continued up to 60°C, where the mobile phase became very predominant. At higher temperatures, only the mobile-phase peaks were seen with a further decrease in the $\Delta\nu_q$. All the changes observed were completely reversible, as seen by the appearance of reproducible ^{2}H NMR peak patterns during heating, cooling, and reheating the samples in the spectrometer to any given temperature.

Electron Microscopy. Figure 6 shows representative thin-section electron micrographs of the lipid mixtures used in the present study. Bilayer configuration of lipids in the mixtures used for NMR experiments was confirmed by the laminar patterns seen in the electron micrographs. Ceramide-containing mixtures formed bilayers that showed some distinct patterns. Figure 6A shows regions where there were repeat units of three bilayers, bounded by major–minor–minor–major electron-dense bands. The thickness of this repeat unit was 13.1 nm. Electron-dense patterns with repeat distances of 12 and 12.8 nm have been reported in thin-section electron micrographs (EM) of SC (24,25). However,

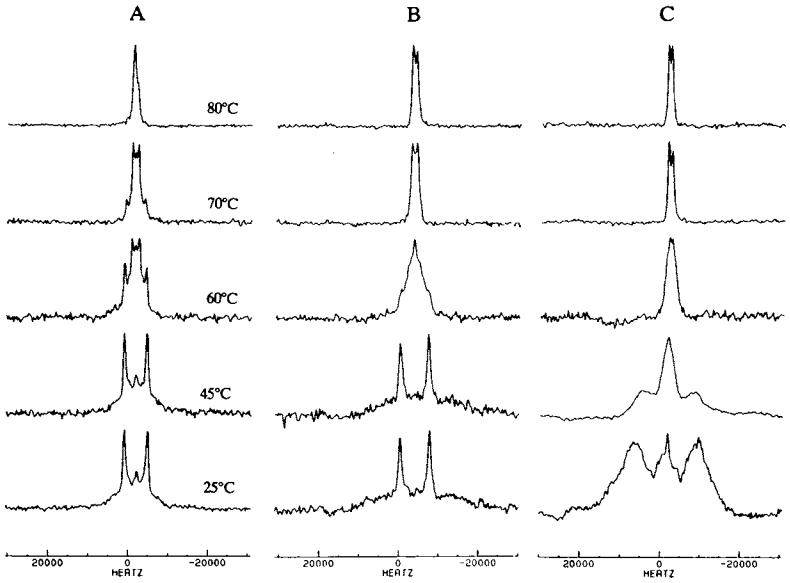

Fig. 3. ^2H NMR spectra of ω-CD_3 palmitic acid intercalated in bilayers formed from mixtures 1–3 shown in Table I at different temperatures. The mixtures were 50% by weight of lipid and 50% water. (A) Mixture 1. (B) Mixture 2, number of scans (NS) = 16,000 at 25°C and NS = 8000 at higher temperatures. (C) Mixture 3: NS = 120,000 at 25°C, NS = 40,000 at 45°C, and NS = 8000 at higher temperatures. Spectral conditions are described under Materials and Methods.

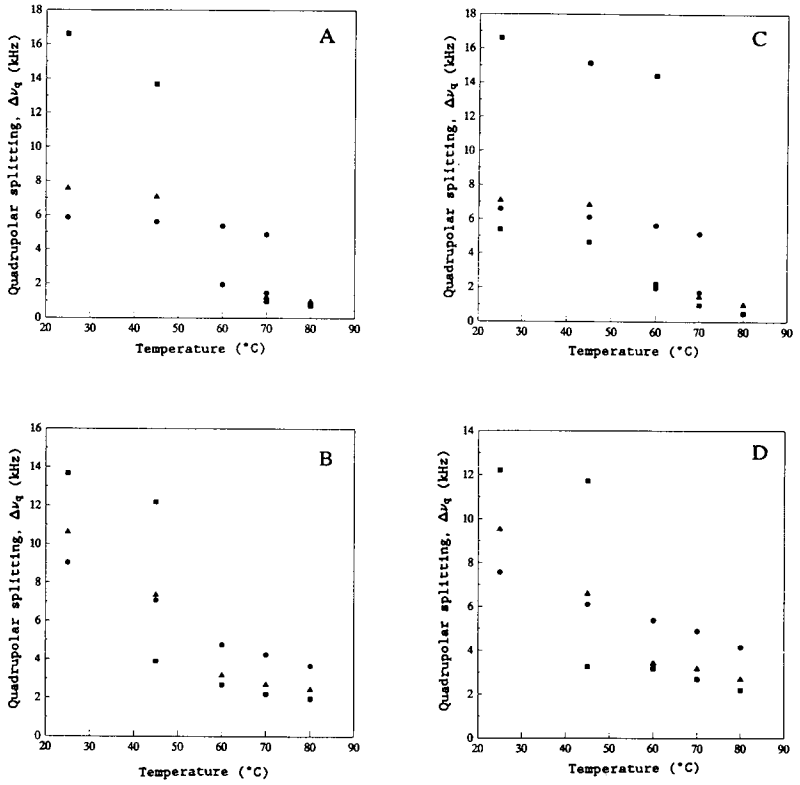

Fig. 4. Quadrupolar splitting ($\Delta\nu_q$) of ω-CD_3 as a function of temperature. (A, C) Ceramide-containing mixtures: 38% ceramides, 38% cholesterol, 19% palmitic acid, and 5% cholesteryl sulfate (●); 57% ceramides, 19% cholesterol, 19% palmitic acid, and 5% cholesteryl sulfate (▲); and 76% ceramides, 19% palmitic acid, and 5% cholesteryl sulfate (■). (B, D) DPPC-containing mixtures: 38% DPPC, 38% cholesterol, 19% palmitic acid, and 5% cholesteryl sulfate (●); 57% DPPC, 19% cholesterol, 19% palmitic acid, and 5% cholesteryl sulfate (▲); and 76% DPPC, 19% palmitic acid, and 5% cholesteryl sulfate (■). (A, B) Fifty percent by weight of lipid and 50% water; (C, D) 75% by weight of lipid and 25% water.

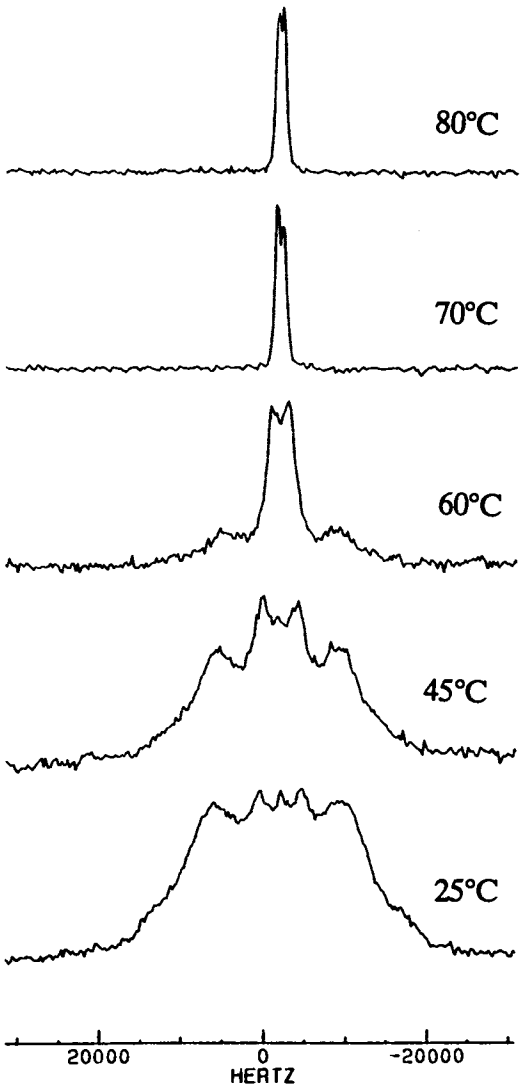

Fig. 5. ^{2}H NMR spectra of mixture 3 at different temperatures. The mixture was 75% by weight of lipid and 25% water. Two pairs of quadrupolar peaks from 25 to 60°C suggest phase separation at a low water content.

the pattern seen in Fig. 6A is different from that reported in native SC (24,25). The major–minor–minor–major electron-dense bands seen in Fig. 6A are similar to the pattern that was observed in the native SC that had been heated to 80°C (17). In the present study also, the samples were heated to 80°C during sample preparation for ^{2}H NMR experiments. The DPPC-containing mixtures formed bilayers that appeared as evenly spaced electron-dense bands with a spacing of 3.84 nm, as shown in Fig. 6B.

DISCUSSION

^{2}H NMR spectroscopy has been shown to be a powerful technique for the investigation of membrane structure and has yielded useful information on the dynamics of lipid molecules in phospholipid bilayers (21,22,26). The results from the present study indicate that deuterated palmitic acid intercalated in bilayers formed by the SC lipids, as well as the DPPC-containing mixtures, can give rise to symmetric powder pattern ^{2}H NMR spectra in the gel phase. We have used this observation to obtain some information on the fluidity of lipid bilayers formed by stratum corneum lipid mixtures near the polar head group and near the end of the acyl chain.

Both the line-shape and the magnitude of $\Delta\nu_q$ for the α-CD_2, as seen in Fig. 1 and Table II, indicated the presence of palmitic acid in lamellar form in mixtures 1–6. The bilayer configuration of the lipid mixtures was confirmed by thin-section electron microscopy. Palmitic acid powder gave a powder pattern with a $\Delta\nu_q$ of 116.7 kHz and a S_{CD} of 0.915, which did not change even after hydrating the palmitic acid in water, as shown in Fig. 2. This is close to the theoretical maximum of 1 for S_{CD} in a rigid crystalline system. The smaller $\Delta\nu_q$ reported in Table II suggest therefore that the palmitic acid molecules were not present in the rigid crystalline form. In the bilayers formed by lipid mixtures shown in Table I, palmitic acid was intercalated with bulkier molecules and only every fifth molecule was palmitic acid. This would prevent close packing such as that present in hydrated palmitic acid.

The ceramide-containing systems have slightly smaller $\Delta\nu_q$ and S_{CD} than the DPPC-containing mixtures, indicating an increase in fluidity near the polar head-group region on

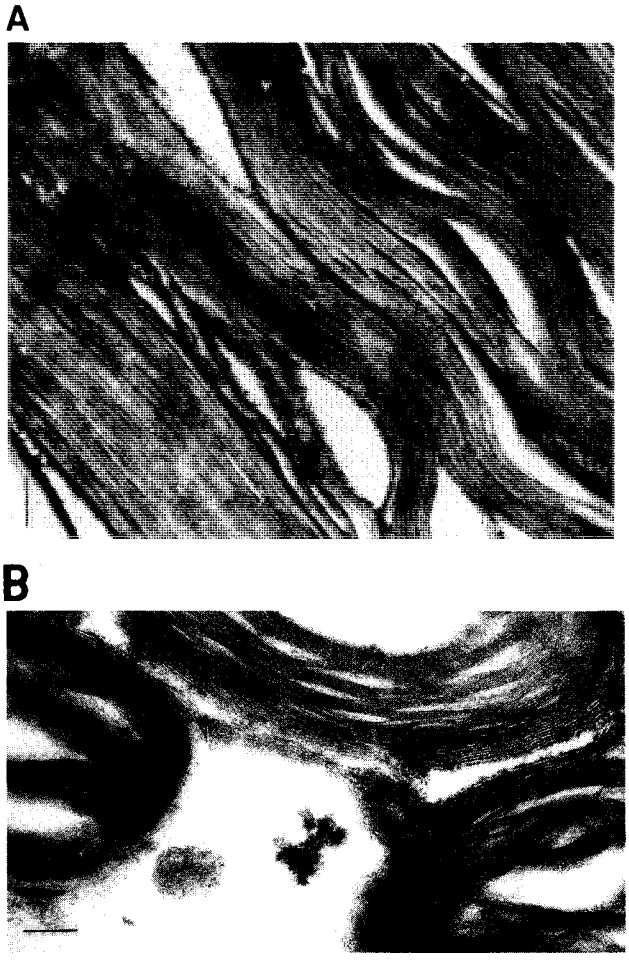

Fig. 6. Thin-section electron micrographs of the lipid mixtures shown in Table I. (A) Mixture 1. Repeat units of three bilayers bounded by major–minor–minor–major electron-dense bands are highlighted by white arrowheads. Bar = 100 nm. (B) Mixture 4. Bilaminar leaflets with a separation of 3.84 nm indicate the presence of bilayer structures. Bar = 100 nm. The samples were fixed in 0.2% RuO_4, as described under Materials and Methods.

replacing DPPC by ceramides. This was completely unexpected, as the ceramides have been shown to promote condensation in the head-group region through lateral hydrogen bonding (27). A closer examination of the orientation of the acyl chains and the head-group regions in ceramides and DPPC reveals that the head group of the ceramide molecule is more rigid. The amide group of the ceramide has been suggested to dictate the conformation of the entire molecule (27). This rigid group, made up of six atoms, has been shown to form a planar conformation and adopt a perpendicular orientation with respect to the acyl chain axes (27). This facilitates lateral hydrogen bonding between the hydroxyl groups of the ceramide with adjacent ceramides, as well as other molecules. When a free fatty acid is intercalated with ceramides in the bilayer, the carboxyl group would be H-bonded with the hydroxyl groups of the ceramides. While this could promote condensation of the head groups, the rigid, planar amide group would in fact disrupt the close packing of the methylenes in the immediate vicinity of the head groups. This could account for the small decrease in the S_{CD} for the α-CD_2 of palmitic acid in bilayers containing ceramides compared to the DPPC-containing bilayers.

Another interesting aspect of the spectra shown in Fig. 1 is the effect of changing the ratio of cholesterol to ceramides or DPPC. Cholesterol is known for its ability to fluidize rigid bilayers as well as for its ability to condense fluid bilayers (28). In the present study, all the mixtures were in the rigid gel phase. Gel-to-liquid crystalline transition of the lipid lamellae of SC has been shown to occur at around 60°C (11). Mixtures 1 and 4, with the largest amount of cholesterol, were more fluid than other mixtures, as judged from the peak shape in Fig. 1 and S_{CD} values in Table II.

Mixture 3 did not give a symmetric powder pattern after repeated attempts with several samples. The spectrum shown in Fig. 1C resembles a powder pattern with a nonzero asymmetry parameter. It would require a complex lineshape analysis in the form of spectral simulation before we could determine the value for the asymmetry parameter. It is equally informative, however, to visualize the mechanism of molecular motion that could give rise to such an asymmetric spectrum. The asymmetry parameter (η) is defined as the difference between the electric field gradient along the two minor axes, X and Y, with Z being defined as the major axis along the acyl chain of the lipid molecule in a bilayer structure (21,22). η for the C–D bond is usually very small and can be taken to be zero (22). However, when palmitic acid molecules are intercalated with high amounts of ceramides, as in mixture 3 (76 mol%), an extended network of lateral hydrogen-bonding could induce some asymmetry in the reorientation of the palmitic acid molecules along their acyl chain axes. This would result in a non-axially symmetric averaging of the quadrupole splittings corresponding to the different orientations of the C–D bond in these bilayers. Comparison of Figs. 1C and F, as well as Figs. 1B and E, shows that this asymmetry is more pronounced in the ceramide-containing mixtures. Thus the spectrum with a nonzero asymmetry parameter for the sample containing 76 mol% of ceramides is the first spectroscopic evidence for H-bonding in the ceramide-containing bilayers and is in agreement with the results from the monolayer studies of ceramides (29). H-bonding involving the hydroxyl groups of ceramides has been suggested to govern the barrier properties of bilayers made up of ceramides, such as that of SC (9).

The results from the lipid mixtures containing the ω-CD_3 palmitic acid provide some insight into the fluidity of the hydrocarbon interior of these bilayers. The $\Delta\nu_q$ for the ω-CD_3 palmatic acid in mixtures 1 and 2 are smaller than the corresponding DPPC-containing mixtures 4 and 5 at room temperature, as shown in Fig. 4. Mixture 3, which contains 76 mol% of ceramides, has a $\Delta\nu_q$ larger than mixture 6. While the DPPC-containing mixtures show a gradual increase in the $\Delta\nu_q$ with the decrease in cholesterol content in the gel phase, the ceramide-containing mixtures show an abrupt increase in the $\Delta\nu_q$ when the cholesterol content is zero, suggesting a greater effect of cholesterol on the ceramide-containing mixtures.

The increase in the fluidity of ω-CD_3 with increasing amounts of cholesterol, both in the ceramide- and in the DPPC-containing mixtures at room temperature, could be explained in terms of a separate cholesterol-rich mobile phase into which the fatty acid could have partitioned. However, as the temperature was raised, the fluidity of the ω-CD_3 actually increased with decreasing amounts of cholesterol in all the mixtures. This is in accordance with the well-known dual role of cholesterol in lipid bilayers, whereby cholesterol increases the fluidity of bilayers in the rigid gel phase and condenses the bilayers in the liquid-crystalline phase (28). The crossover of the $\Delta\nu_q$ values seen in Fig. 4, as the amount of cholesterol is decreased, as a function of temperature illustrates this dual role of cholesterol.

One interesting aspect of the variable temperature spectra of the ceramide-containing mixtures is the dramatic change seen in the shape of the spectra for mixture 2, as shown in Fig. 3B. As the temperature was raised from 25 to 80°C, the powder pattern spectrum changed to a highly asymmetric spectrum at 60°C, just around the gel–liquid crystalline phase transition temperature of the SC lipids (11). At higher temperatures, the pattern reverted to a highly symmetric powder pattern with a much reduced $\Delta\nu_q$. This is somewhat similar to the temperature-dependent change in ^2H NMR spectral shape reported for *N*-palmitoylgalactocerebroside (30). In that study, a triangular peak was observed for the 6,6-D_2 *N*-palmitoylgalactocerebroside at 55°C and was attributed to "hopping" between two sites resulting from gauche–trans isomerization. It is very likely that similar gauche–trans isomerization, occurring in the ceramide-containing system in the limit of fast exchange on the deuterium NMR time scale, caused this asymmetric peak at 60°C. The reason for this behavior being observed in mixture 2 alone is not clear at the present moment, although similar asymmetric peaks might be appearing for mixtures 1 and 3 at temperatures other than those used for recording the spectra in the present study.

In conclusion, the results from the present study provide the first spectroscopic evidence for head-group condensation in the ceramide-containing mixtures, presumably resulting from extensive H-bonding involving the hydroxyl groups of these molecules. The formation of the hexagonal phase by the ceramide-containing lipid mixtures reported recently (23) is confirmed by the results from the present study. While mixture 1 used in the present study was a close approximation to the *in situ* SC lipid composition, the low

cholesterol-containing mixtures did not resemble the *in situ* composition. Nevertheless, the findings from the present study regarding the polymorphism in these relatively nonpolar lipid mixtures is significant to the understanding of SC membrane function. The effective barrier property of the SC intercellular lipid lamellae has been attributed to the highly ordered bilayer structures in the intercellular space of the SC. The results from the present study suggest that the ceramide-containing lipid mixtures can be induced to form the H_{II} phase that would be highly permeable due to its disordered hydrocarbon core, compared to the highly ordered bilayer phase. Such a reversible L_α–H_{II} phase transition could be induced *in situ* by the addition of molecules of suitable geometry, thereby enhancing the percutaneous penetration of drugs. Understanding the phase behavior of the heterogeneous lipid mixtures of SC using model systems is important in understanding the factors that influence the barrier function of SC of the mammalian skin.

ACKNOWLEDGMENTS

NMR spectra were acquired using the Bruker MSL-300 spectrometer in the High-Field NMR facility at the University of Iowa. This study was supported in part by Grant AR 32374 from the Untied States Public Health Service.

REFERENCES

1. A. G. Matoltsy. Keratinization. *J. Invest. Dermatol.* 67:20–25 (1976).
2. A. S. Michaels, S. K. Chandrasekaran, and J. E. Shaw. Drug permeation through human skin: Theory and in vitro experimental measurement. *Am. Inst. Chem. Eng. J.* 21:985–996 (1975).
3. P. M. Elias. Epidermal lipids, barrier function, and desquamation. *J. Invest. Dermatol.* 80(Suppl.):44s–49s (1983).
4. G. M. Gray, R. J. White, R. H. William, and H. J. Yardley. Lipid composition of the superficial stratum corneum cells of pig epidermis. *Br. J. Dermatol.* 106:59–63 (1982).
5. H. J. Yardley and R. Summerly. Lipid composition and metabolism in normal and diseased epidermis. *Pharmacol. Ther.* 13:357–383 (1981).
6. P. W. Wertz, D. C. Swartzendruber, K. C. Madison, and D. T. Downing. Composition and morphology of epidermal cyst lipids. *J. Invest. Dermatol.* 89:419–425 (1987).
7. P. W. Wertz, W. Abraham, L. Landmann, and D. T. Downing. Preparation of liposomes from stratum corneum lipids. *J. Invest. Dermatol.* 87:582–584 (1986).
8. W. Abraham, P. W. Wertz, and D. T. Downing. Effect of epidermal acylglucosylceramides and acylceramides on the morphology of liposomes prepared from stratum corneum lipids. *Biochim. Biophys. Acta* 939:403–408 (1988).
9. W. Abraham and D. T. Downing. Preparation of model membranes for skin permeability studies using stratum corneum lipids. *J. Invest. Dermatol.* 93:809–813 (1989).
10. B. F. Van Duzee. Thermal analysis of human stratum corneum. *J. Invest. Dermatol.* 65:404–408 (1975).
11. G. M. Golden, D. B. Guzek, R. R. Harris, J. E. McKie, and R. O. Potts. Lipid thermotropic transitions in human stratum corneum. *J. Invest. Dermatol.* 86:255–259 (1986).
12. K. Knutson, R. O. Potts, D. B. Guzek, G. M. Golden, J. E. McKie, W. J. Lambert, and W. I. Higuchi. Macro- and molecular-physical considerations in understanding drug transport in the stratum corneum. *J. Control. Release* 2:67–87 (1985).
13. G. M. Golden, D. B. Guzek, A. H. Kennedy, J. E. McKie, and R. O. Potts. Stratum corneum lipid phase transition and water barrier properties. *Biochemistry* 26:2382–2388 (1987).
14. S. J. Rehfeld, W. Z. Plachy, M. Williams, and P. M. Elias. Calorimetric and electron spin resonance examination of lipid phase transitions in human stratum corneum: Molecular basis for normal cohesion and abnormal desquamation in recessive X-linked ichthyosis. *J. Invest. Dermatol.* 91:499–505 (1988).
15. K. C. Madison, D. C. Swartzendruber, P. W. Wertz, and D. T. Downing. Presence of intact intercellular lipid lamellae in the upper layers of stratum corneum. *J. Invest. Dermatol.* 88:714–718 (1987).
16. L. Landmann. The epidermal permeability barrier. *Anat. Embryol.* 178:1–13 (1988).
17. D. C. Swartzendruber, P. W. Wertz, D. J. Kitko, K. C. Madison, and D. T. Downing. Molecular models of the intercellular lipid lamellae in mammalian stratum corneum. *J. Invest. Dermatol.* 92:251–257 (1989).
18. S. H. White, D. Mirejovsky, and G. I. King. Structure of lipid domains and corneocyte envelopes of murine stratum corneum. An X-ray diffraction study. *Biochemistry* 27:3725–3732 (1988).
19. D. C. Swartzendruber, D. J. Kitko, P. W. Wertz, K. C. Madison, and D. T. Downing. Isolation of corneocyte envelopes from porcine epidermis. *Arch. Dermatol. Res.* 280:424–429 (1988).
20. J. H. Davis, K. R. Jeffrey, M. Bloom, and M. I. Valic. Quadrupolar echo deuteron magnetic resonance spectroscopy in ordered hydrocarbon chains. *Chem. Phys. Lett.* 42:390–394 (1976).
21. J. Seelig. Deuterium magnetic resonance: Theory and application to lipid membranes. *Q. Rev. Biophys.* 10:353–418 (1977).
22. J. H. Davis. The description of membrane lipid conformation, order and dynamics by ^{2}H NMR. *Biochim. Biophys. Acta* 73:117–171 (1983).
23. W. Abraham and D. T. Downing. Deuterium NMR investigation of polymorphism in stratum corneum lipids. *Biochim. Biophys. Acta* 1068:189–194 (1991).
24. R. M. Lavker. Membrane coating granules: The fate of the discharged lamellae. *J. Ultrastruct. Res.* 55:79–96 (1976).
25. K. C. Madison, D. C. Swartzendruber, P. W. Wertz, and D. T. Downing. Presence of intact intercellular lipid lamellae in the upper layers of the stratum corneum. *J. Invest. Dermatol.* 88:714–718 (1987).
26. A. Seelig and J. Seelig. Lipid conformation in model membranes and biological membranes. *Q. Rev. Biophys.* 13:19–61 (1980).
27. I. Pascher. Molecular arrangements in sphingolipids. Conformation and hydrogen bonding of ceramides and their implication on membranes stability and permeability. *Biochim. Biophys. Acta* 455:433–451 (1976).
28. P. L. Yeagle. Cholesterol and the cell membrane. *Biochim. Biophys. Acta* 822:267–287 (1985).
29. H. Lofgren and I. Pascher. Molecular arrangements of sphingolipids. The monolayer behaviour of ceramides. *Chem. Phys. Lipids* 20:273–284 (1977).
30. R. L. Smith and E. Oldfield. Dynamic structure of membranes by deuterium NMR. *Science* 225:280–288 (1984).